



<http://www.diva-portal.org>

Preprint

This is the submitted version of a paper presented at *IEEE International Conference on Fuzzy Systems (FUZZ-IEEE 2019), New Orleans, USA, June 23 - 26, 2019*.

Citation for the original published paper:

Palm, R., Lilienthal, A. (2019)

Gaussian Noise and the Intersection Problem in Human-Robot Systems: Analytical and Fuzzy Approach

In: *2019 IEEE International Conference on Fuzzy Systems (FUZZ-IEEE)*, 8858796

(pp. 1-6). IEEE

<https://doi.org/10.1109/FUZZ-IEEE.2019.8858796>

N.B. When citing this work, cite the original published paper.

Permanent link to this version:

<http://urn.kb.se/resolve?urn=urn:nbn:se:oru:diva-79734>

Gaussian noise and the intersection problem in Human-Robot Systems - analytical and fuzzy approach

Rainer Palm
AASS
Oerebro university
Oerebro, Sweden
rub.palm@t-online.de

Achim Lilienthal
AASS
Oerebro university
Oerebro, Sweden
achim.lilienthal@oru.se

Abstract—In this paper the intersection problem in human-robot systems with respect to noisy information is discussed. The interaction between humans and mobile robots in shared areas requires a high level of safety especially at the intersections of trajectories. We discuss the intersection problem with respect to noisy information on the basis of an analytic geometrical model and its TS fuzzy version. The transmission of a 2-dimensional Gaussian noise signal, in particular information on human and robot orientations, through a non-linear static system and its fuzzy version, will be described. We discuss the problem: Given the parameters of the input distributions, find the parameters of the output distributions.

I. INTRODUCTION

Activities of human operators and mobile robots in shared areas require high attention regarding system stability and safety. Planning of mobile robot tasks, navigation and obstacle avoidance were main research activities during many years [1], [2], [3]. The simultaneous use of the same workspace requires an adaptation of the behavior of both human agents and robots to facilitate successful collaboration or to support separate work for both. In this connection, the recognition of human intentions to reach at a certain target is an important aspect which has been reported by [4], [5], [6]. Bruce et al address a planned human-robot rendezvous at an intersection zone [7]. Human-like sensors/systems allow for easier and more natural human-robot interaction because they share their principle of operation with natural systems [8], [9], [10]. Based on an estimation of positions and orientations of robot and human, the intersections of intended linear trajectories of robot and human are computed. Due to system uncertainties and observation noise the intersection points are corrupted with noise as well. Depending on the distance between human and robot, uncertainties in human/robot orientations with standard deviations of more than one degree may lead to high uncertainties at the intersection points. Therefore, for the sake of human safety and for an effective human-robot collaboration it is essential to predict uncertainties at possible crossing points. The relationship between human/robot position and orientation and the intersection coordinates is nonlinear, but can be linearized under certain restrictions. This is especially true if

we only consider the linear part of correlation between input and output of a nonlinear transfer element [11], [12]. This is also valid for small standard deviations at the input. For fuzzy systems two main directions to deal with uncertain system inputs are the following: One direction is the processing of fuzzy inputs (inputs that are fuzzy sets) in fuzzy systems [13], [14]. Another direction is the fuzzy reasoning with probabilistic inputs [15] and the transformation of probabilistic distributions into fuzzy sets [16]. Both approaches fail more or less to solve the practical problem of the processing of a probabilistic distribution through a static fuzzy system. The content and the contribution of this paper is the direct task: given the parameters of Gaussian distributions at the input of a fuzzy system, find the corresponding parameters of the output distributions. The inverse task would be: Given the output distribution parameters, find the input distribution parameters. An application is the bearing task for intersections of possible trajectories emanating from different positions for the same target. In the following we restrict our consideration to the direct task and the static one-robot one-human-case in order to show the general problems and difficulties. Cases that are relevant for adaptation of velocities and directions of motions have already been described in [6], [3].

The paper is organized as follows. Section II deals with Gaussian noise and the bearing problem in general and its analytical approach. Section III deals with the corresponding fuzzy approach. In section IV the extension from 2 inputs to 6 inputs is discussed. Section V deals with simulations to show the influence of the resolution of the fuzzy system onto the accuracy at the system output. Finally, section VI concludes the paper.

II. GAUSSIAN NOISE AND THE BEARING PROBLEM

A. Computation of intersections - analytical approach

The following computation deals with the intersection (x_c, y_c) of two linear paths in a plane along which robot and human will move. Let $\mathbf{x}_H = (x_H, y_H)$ and $\mathbf{x}_R = (x_R, y_R)$

be the position of human and robot and ϕ_H and ϕ_R their orientation angles (see Fig. 1). Then we have the relations

$$\begin{aligned} x_H &= x_R + d_{RH} \cos(\phi_R + \delta_R) \\ y_H &= y_R + d_{RH} \sin(\phi_R + \delta_R) \\ x_R &= x_H + d_{RH} \cos(\phi_H + \delta_H) \\ y_R &= y_H + d_{RH} \sin(\phi_H + \delta_H) \end{aligned} \quad (1)$$

where positive angles δ_H and δ_R are measured from the y coordinates counterclockwise. The variables \mathbf{x}_H , \mathbf{x}_R , ϕ_R , δ_H , δ_R , d_{RH} and the angle γ are supposed to be measurable. The unknown orientation angle ϕ_H can be computed by

$$\phi_H = \arcsin((y_H - y_R)/d_{RH}) - \delta_H + \pi \quad (2)$$

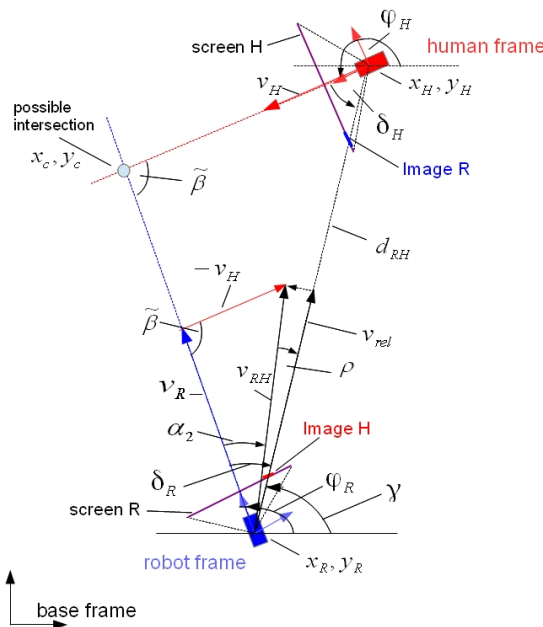


Fig. 1. Human-robot scenario

Then after some substitutions we get the coordinates x_c and y_c straight forward

$$\begin{aligned} x_c &= \frac{A - B}{\tan \phi_R - \tan \phi_H} \\ y_c &= \frac{A \tan \phi_H - B \tan \phi_R}{\tan \phi_R - \tan \phi_H} \\ A &= x_R \tan \phi_R - y_R \\ B &= x_H \tan \phi_H - y_H \end{aligned} \quad (3)$$

Rewriting (3) leads to a form that can be used for the fuzzification of (3)

$$\begin{aligned} x_c &= \left(x_R \frac{\tan \phi_R}{G} - y_R \frac{1}{G} \right) - \left(x_H \frac{\tan \phi_H}{G} - y_H \frac{1}{G} \right) \\ y_c &= \left(x_R \frac{\tan \phi_R \tan \phi_H}{G} - y_R \frac{\tan \phi_H}{G} \right) \\ &\quad - \left(x_H \frac{\tan \phi_H \tan \phi_R}{G} - y_H \frac{\tan \phi_R}{G} \right) \\ G &= \tan \phi_R - \tan \phi_H \end{aligned} \quad (4)$$

from which we see that $\mathbf{x}_c = (x_c, y_c)^T$ is linear in $\mathbf{x}_{RH} = (x_R, y_R, x_H, y_H)^T$

$$\mathbf{x}_c = A_{RH} \cdot \mathbf{x}_{RH} \quad (5)$$

where

$$A_{RH} = f(\phi_R, \phi_H) = \frac{1}{G} \begin{pmatrix} \tan \phi_R & -1 & -\tan \phi_H & 1 \\ \tan \phi_R \tan \phi_H & -\tan \phi_H & -\tan \phi_R \tan \phi_H & \tan \phi_H \end{pmatrix}$$

The TS-fuzzy approximation of (5) (see [3]) is given by

$$\mathbf{x}_c = \sum_{i,j} w_i(\phi_R) w_j(\phi_H) \cdot A_{RH,i,j} \cdot \mathbf{x}_{RH} \quad (6)$$

$w_i(\phi_R), w_j(\phi_H) \in [0, 1]$ are normalized membership functions with $\sum_i w_i(\phi_R) = 1$ and $\sum_j w_j(\phi_H) = 1$. The following paragraph deals with the accuracy of the computed intersection in the case of distorted orientation information.

B. Transformation of Gaussian distributions

1) *General considerations:* Let us consider a static nonlinear system

$$\mathbf{z} = F(\mathbf{x}) \quad (7)$$

with 2 inputs $\mathbf{x} = (x_1, x_2)^T$ and 2 outputs $\mathbf{z} = (z_1, z_2)^T$. Let further the uncorrelated Gaussian distributed inputs x_1 and x_2 be described by the 2-dim distribution

$$f_{x_1, x_2} = \frac{1}{2\pi\sigma_{x_1}\sigma_{x_2}} \exp\left(-\frac{1}{2}\left(\frac{e_{x_1}^2}{\sigma_{x_1}^2} + \frac{e_{x_2}^2}{\sigma_{x_2}^2}\right)\right) \quad (8)$$

where $e_{x_i} = x_i - \bar{x}_i$, \bar{x}_i - mean(x_i), σ_{x_i} - standard deviation x_i , $i = 1, 2$.

The question arises how the output signals z_1 and z_2 are distributed in order to obtain their standard deviations and the correlation coefficient between the outputs. For linear systems Gaussian distributions are linearly transformed which means that the output signals are also Gaussian distributed. In general, this does not apply for nonlinear system as in our case. However, if we assume the input standard deviations small enough then we can construct local linear transfer functions for which the output distributions are nearly Gaussian distributed but correlated in general.

$$\begin{aligned} f_{z_1, z_2} &= \frac{1}{2\pi\sigma_{z_1}\sigma_{z_2}\sqrt{1-\rho_{z_{12}}^2}} \cdot \\ &\quad \exp\left(-\frac{1}{2(1-\rho_{z_{12}}^2)}\left(\frac{e_{z_1}^2}{\sigma_{z_1}^2} + \frac{e_{z_2}^2}{\sigma_{z_2}^2} - \frac{2\rho_{z_{12}}e_{z_1}e_{z_2}}{\sigma_{z_1}\sigma_{z_2}}\right)\right) \end{aligned} \quad (9)$$

$\rho_{z_{12}}$ - correlation coefficient.

2) *Differential approach:* Function F can be described by individual smooth and nonlinear static transfer functions

$$\begin{aligned} z_1 &= f_1(x_1, x_2) \\ z_2 &= f_2(x_1, x_2) \end{aligned} \quad (10)$$

Linearization of (10) yields

$$\mathbf{dz} = \tilde{J} \cdot \mathbf{dx} \quad \text{or} \quad \mathbf{e}_z = \tilde{J} \cdot \mathbf{e}_x \quad (11)$$

with

$$\begin{aligned} \mathbf{e}_z &= (e_{z_1}, e_{z_2})^T \quad \text{and} \quad \mathbf{e}_x = (e_{x_1}, e_{x_2})^T \\ \mathbf{dz} &= (dz_1, dz_2)^T \quad \text{and} \quad \mathbf{dx} = (dx_1, dx_2)^T \end{aligned}$$

$$\tilde{J} = \begin{pmatrix} \partial f_1 / \partial x_1, \partial f_1 / \partial x_2 \\ \partial f_2 / \partial x_1, \partial f_2 / \partial x_2 \end{pmatrix}$$

3) *Specific approach to the intersection:* Beside the exact solution (4) it is recommended to search for a differential approach of the intersection problem. This comes into play when the contributing agents, robot and human, change their directions of motion. Another aspect is to quantify the uncertainty of \mathbf{x}_c in the presence of uncertainty in angles ϕ_R and ϕ_H or in $\mathbf{x}_{RH} = (x_R, y_R, x_H, y_H)^T$.

Differentiating of (4) with $\mathbf{x}_{RH} = \text{const.}$ yields

$$\begin{aligned} \dot{\mathbf{x}}_c &= \tilde{J} \cdot \dot{\phi} \\ \dot{\phi} &= (\dot{\phi}_R \quad \dot{\phi}_H)^T; \quad \tilde{J} = \begin{pmatrix} \tilde{J}_{11} & \tilde{J}_{12} \\ \tilde{J}_{21} & \tilde{J}_{22} \end{pmatrix} \end{aligned} \quad (12)$$

where

$$\begin{aligned} \tilde{J}_{11} &= (-\tan \phi_H \quad 1 \quad \tan \phi_H \quad -1) \frac{\mathbf{x}_{RH}}{G^2 \cdot \cos^2 \phi_R} \\ \tilde{J}_{12} &= (\tan \phi_R \quad -1 \quad -\tan \phi_R \quad 1) \frac{\mathbf{x}_{RH}}{G^2 \cdot \cos^2 \phi_H} \\ \tilde{J}_{21} &= \tilde{J}_{11} \cdot \tan \phi_H \\ \tilde{J}_{22} &= \tilde{J}_{12} \cdot \tan \phi_R \end{aligned}$$

4) *Output distribution:* To obtain the distribution f_{z_1, z_2} of the output signal we invert (11) and substitute the entries of \mathbf{e}_x into (8)

$$\mathbf{e}_x = J \cdot \mathbf{e}_z \quad (13)$$

with $J = \tilde{J}^{-1}$ and

$$J = \begin{pmatrix} J_{11} & J_{12} \\ J_{21} & J_{22} \end{pmatrix} = \begin{pmatrix} \mathbf{j}_{xz} \\ \mathbf{j}_{yz} \end{pmatrix} \quad (14)$$

where $\mathbf{j}_{xz} = (J_{11}, J_{12})$ and $\mathbf{j}_{yz} = (J_{21}, J_{22})$. Entries J_{ij} are the result of the inversion of \tilde{J} . From this substitution which we get

$$\begin{aligned} f_{z_1, z_2} &= K_{x_1, x_2} \cdot \\ \exp(-\frac{1}{2} \cdot \mathbf{e}_z^T \cdot (\mathbf{j}_{x_1, z}^T, \mathbf{j}_{x_2, z}^T) \cdot S_x^{-1} \cdot \begin{pmatrix} \mathbf{j}_{x_1, z} \\ \mathbf{j}_{x_2, z} \end{pmatrix} \cdot \mathbf{e}_z) \end{aligned} \quad (15)$$

where $K_{x_1, x_2} = \frac{1}{2\pi\sigma_{x_1}\sigma_{x_2}}$ and

$$S_x^{-1} = \begin{pmatrix} \frac{1}{\sigma_{x_1}^2}, 0 \\ 0, \frac{1}{\sigma_{x_2}^2} \end{pmatrix} \quad (16)$$

The exponent of (15) is rewritten into

$$\begin{aligned} xpo &= -\frac{1}{2} \cdot [e_{z_1}^2 \left(\frac{J_{11}^2}{\sigma_{x_1}^2} + \frac{J_{21}^2}{\sigma_{x_2}^2} \right) + e_{z_2}^2 \left(\frac{J_{12}^2}{\sigma_{x_1}^2} + \frac{J_{22}^2}{\sigma_{x_2}^2} \right) + \\ &\quad 2 \cdot e_{z_1} e_{z_2} \left(\frac{J_{11} J_{12}}{\sigma_{x_1}^2} + \frac{J_{21} J_{22}}{\sigma_{x_2}^2} \right)] \end{aligned} \quad (17)$$

Let

$$\begin{aligned} A &= \left(\frac{J_{11}^2}{\sigma_{x_1}^2} + \frac{J_{21}^2}{\sigma_{x_2}^2} \right); \quad B = \left(\frac{J_{12}^2}{\sigma_{x_1}^2} + \frac{J_{22}^2}{\sigma_{x_2}^2} \right) \\ C &= \left(\frac{J_{11} J_{12}}{\sigma_{x_1}^2} + \frac{J_{21} J_{22}}{\sigma_{x_2}^2} \right) \end{aligned} \quad (18)$$

then a comparison of xpo in (17) and the exponent in (9) yields

$$\begin{aligned} \frac{1}{(1 - \rho_{z_{12}}^2)} \frac{1}{\sigma_{z_1}^2} &= A; \quad \frac{1}{(1 - \rho_{z_{12}}^2)} \frac{1}{\sigma_{z_2}^2} = B \\ \frac{-2\rho_{z_{12}}}{(1 - \rho_{z_{12}}^2)} \frac{1}{\sigma_{z_1} \sigma_{z_2}} &= 2C \end{aligned} \quad (19)$$

from which we finally get the correlation coefficient $\rho_{z_{12}}$ and the standard deviations σ_{z_1} and σ_{z_2}

$$\begin{aligned} \rho_{z_{12}} &= -\frac{C}{\sqrt{AB}} \\ \frac{1}{\sigma_{z_1}^2} &= A - \frac{C^2}{B}; \quad \frac{1}{\sigma_{z_2}^2} = B - \frac{C^2}{A} \end{aligned} \quad (20)$$

So once we have obtained the parameters of the input distribution and the mathematical expression for the transfer function $F(x, y)$ we get the output distribution parameters straight forward.

III. FUZZY APPROACH

The previous presentation shows that the computation of the output distribution can be of high effort which might be problematic especially in the on-line case. Provided that an analytical representation (7) is available then we have two methods to build a TS fuzzy model.

Method 1:

Based on values A_i , B_i and C_i at predefined orientations $\mathbf{x}_i = (x_1, x_2)_i^T = (\phi_R, \phi_H)_i^T$ we formulate the following rules

$$R_i : \quad (21)$$

$$\begin{aligned} \text{IF } \mathbf{x}_i &= \mathbf{X}_i \quad \text{THEN} \quad \rho_{z_{12}} = -\frac{C_i}{\sqrt{A_i B_i}} \\ \text{AND } \frac{1}{\sigma_{z_1}^2} &= A_i - \frac{C_i^2}{B_i} \quad \text{AND} \quad \frac{1}{\sigma_{z_2}^2} = B_i - \frac{C_i^2}{A_i} \end{aligned}$$

where \mathbf{X}_i are fuzzy terms for \mathbf{x}_i , l - number of fuzzy terms, k - number of variables, $k = 2$, $i = 1 \dots n$, $n = l^k$ - number of rules

From this set of rules we obtain

$$\begin{aligned} \rho_{z_{12}} &= -\sum_i w_i(\mathbf{x}) \frac{C_i}{\sqrt{A_i B_i}} \\ \frac{1}{\sigma_{z_1}^2} &= \sum_i w_i(\mathbf{x}) (A_i - \frac{C_i^2}{B_i}) \\ \frac{1}{\sigma_{z_2}^2} &= \sum_i w_i(\mathbf{x}) (B_i - \frac{C_i^2}{A_i}) \end{aligned} \quad (22)$$

$w_i(\mathbf{x}) = \prod_{l=1}^2 w_l(x_l)$, $w_l(x_l) \in [0, 1]$ are weighting functions with $\sum_i w_i(\mathbf{x}) = 1$

Method 2:

Based on values A_i , B_i and C_i at predefined orientations \mathbf{x}_i , $i = 1 \dots n$, n^2 - number of rules we compute the corresponding $\rho_{z_{12}}$, $\frac{1}{\sigma_{z_1}^2}$, $\frac{1}{\sigma_{z_2}^2}$. From this we formulate the following rules

$$\begin{array}{ll} R_i : & \\ \text{IF } \mathbf{x}_i = \mathbf{X}_i & \text{THEN } \rho_{z_{12}} = \rho_{z_{12}} \\ \text{AND } \frac{1}{\sigma_{z_1}^2} = \frac{1}{\sigma_{z_1}^2} & \text{AND } \frac{1}{\sigma_{z_2}^2} = \frac{1}{\sigma_{z_2}^2} \end{array} \quad (23)$$

From (23) we get

$$\begin{aligned} \rho_{z_{12}} &= -\sum_i w_i(\mathbf{x}) \rho_{z_{12}} \\ \frac{1}{\sigma_{z_1}^2} &= \sum_i w_i(\mathbf{x}) \frac{1}{\sigma_{z_1}^2} \\ \frac{1}{\sigma_{z_2}^2} &= \sum_i w_i(\mathbf{x}) \frac{1}{\sigma_{z_2}^2} \end{aligned} \quad (24)$$

Both methods seem to be of equal quality, but simulations show that this is not always the case due to the different levels of computation at which the fuzzy interpolation takes place.

IV. EXTENSION TO 6 INPUTS AND 2 OUTPUTS

A. Non-fuzzy approach

The previous section dealt with two orientation inputs and two intersection position outputs where the position coordinates of robot and human are assumed to be constant. Let us again consider the nonlinear system

$$\mathbf{x}_c = F(\mathbf{x}) \quad (25)$$

where F denotes a nonlinear system. Here we have 6 inputs $\mathbf{x} = (x_1, x_2, x_3, x_4, x_5, x_6)^T$ and 2 outputs $\mathbf{x}_c = (x_c, y_c)^T$. For the bearing problem we get $\mathbf{x} = (\phi_R, \phi_H, x_R, y_R, x_H, y_H)^T$

Let further the uncorrelated Gaussian distributed inputs $x_1 \dots x_6$ be described by the 6-dim distribution

$$f_{x_i} = \frac{1}{(2\pi)^{6/2} |S_x|^{1/2}} \exp(-\frac{1}{2} (\mathbf{e}_x^T S_x^{-1} \mathbf{e}_x)) \quad (26)$$

where $\mathbf{e}_x = (e_{x1}, e_{x2}, \dots, e_{x6})^T$; $\mathbf{e}_x = \mathbf{x} - \bar{\mathbf{x}}$, $\bar{\mathbf{x}}$ - mean(\mathbf{x}), S_x - covariance matrix.

$$S_x = \begin{pmatrix} \sigma_{x_1}^2 & 0 & \dots & 0 \\ 0 & \sigma_{x_2}^2 & \dots & 0 \\ \dots & \dots & \dots & \dots \\ 0 & \dots & 0 & \sigma_{x_6}^2 \end{pmatrix}$$

The output distribution is again described by

$$\begin{aligned} f_{x_c, y_c} &= \frac{1}{2\pi\sigma_{x_c}\sigma_{y_c}\sqrt{1-\rho^2}} \cdot \\ &\exp\left(-\frac{1}{2(1-\rho^2)}(\mathbf{e}_{x_c}^T S_c^{-1} \mathbf{e}_{x_c} - \frac{2\rho e_{x_c} e_{y_c}}{\sigma_{x_c} \sigma_{y_c}})\right) \end{aligned} \quad (27)$$

$$S_c^{-1} = \begin{pmatrix} \frac{1}{\sigma_{x_c}^2}, 0 \\ 0, \frac{1}{\sigma_{y_c}^2} \end{pmatrix} \quad (28)$$

ρ - correlation coefficient.

In correspondence to (7) and (10) function F can be described by

$$x_c = f_1(\mathbf{x}); \quad y_c = f_2(\mathbf{x}) \quad (29)$$

Furthermore we have in correspondence to (12)

$$\mathbf{e}_{x_c} = \tilde{J} \cdot \mathbf{e}_x; \quad \tilde{J} = \begin{pmatrix} \tilde{J}_{11} & \tilde{J}_{12} & \dots & \tilde{J}_{16} \\ \tilde{J}_{21} & \tilde{J}_{22} & \dots & \tilde{J}_{26} \end{pmatrix} \quad (30)$$

where

$$\tilde{J}_{ij} = \frac{\partial f_i}{\partial x_j}, \quad i = 1, 2, \dots, j = 1, \dots, 6 \quad (31)$$

Inversion of (30) leads to

$$\mathbf{e}_x = \tilde{J}^t \cdot \mathbf{e}_{x_c} = J \cdot \mathbf{e}_{x_c} \quad (32)$$

with the pseudo inverse \tilde{J}^t . Renaming $\tilde{J}^t = J$ yields

$$J = \begin{pmatrix} J_{11} & J_{12} \\ \dots & \dots \\ J_{61} & J_{62} \end{pmatrix}; \quad (33)$$

Substituting (30) into (26) we obtain

$$f_{x_c, y_c} = K_{x_c} \exp\left(-\frac{1}{2} (\mathbf{e}_{x_c}^T J^T S_x^{-1} J \mathbf{e}_{x_c})\right) \quad (34)$$

where K_{x_c} represents a normalization of the output distribution and

$$J_{x_c} = J^T S_x^{-1} J = \begin{pmatrix} A & B \\ C & D \end{pmatrix}$$

where

$$\begin{aligned} A &= \sum_{i=1}^6 \frac{1}{\sigma_{x_i}^2} J_{i1}^2; \quad B = \sum_{i=1}^6 \frac{1}{\sigma_{x_i}^2} J_{i1} J_{i2} \\ C &= \sum_{i=1}^6 \frac{1}{\sigma_{x_i}^2} J_{i1} J_{i2}; \quad D = \sum_{i=1}^6 \frac{1}{\sigma_{x_i}^2} J_{i2}^2 \end{aligned} \quad (35)$$

Substitution of (35) into (34) leads with $B = C$ to

$$f_{x_c, y_c} = K_{x_c} \exp\left(-\frac{1}{2} (A e_{x_c}^2 + D e_{y_c}^2 + 2 C e_{x_c} e_{y_c})\right) \quad (36)$$

Comparison of (36) with (27) leads with (33) to

$$\begin{aligned}\rho &= -\frac{C}{\sqrt{AD}} \\ \frac{1}{\sigma_{x_c}^2} &= A - \frac{C^2}{D}; \quad \frac{1}{\sigma_{y_c}^2} = D - \frac{C^2}{A}\end{aligned}\quad (37)$$

which is the counterpart to the 2-dim input case (20).

B. Fuzzy approach

The first step is to compute values A_i , B_i and C_i from (35) at predefined positions/orientations $\mathbf{x} = (x_1, x_2, x_3, x_4, x_5, x_6)^T$. Then, using method 1 we formulate fuzzy rules R_i , according to (21) and (22) with $i = 1 \dots n$, l - number of fuzzy terms, $k = 6$ - number of variables $n = lk$ - number of rules. The same applies for method M2 using rules (23) with subsequent results (24). With such an increase in the number of inputs, one unfortunately sees the problem of an exponential increase in the number of rules, which is associated with a very high computational burden.

For $l = 7$ fuzzy terms for each input variable x_k , $k = 6$ we end up with $n = 7^6$ rules which is much to high to deal with in a reasonable way. So, one has to restrict to a reasonable number of variables at the input of a fuzzy system. This can be done either in a heuristic or systematic way [17] to find out the most influential input variables which is however not the issue of this paper.

V. SIMULATION RESULTS

Based on the human-robot intersection example, the following simulation results show the feasibility to predict uncertainties at possible intersections by using analytical and/or fuzzy models for a static situation. Position/orientation of robot and human are given by $\mathbf{x}_R = (x_R, y_R) = (2, 0)$ m and $\mathbf{x}_H = (x_H, y_H) = (4, 10)$ m and $\phi_R = 1.78$ rad, ($= 102^\circ$), and $\phi_H = 3.69$ rad, ($= 212^\circ$). ϕ_R and ϕ_H are corrupted with Gaussian noise with standard deviations (std) of $\sigma_{\phi_R} = \sigma_{x_1} = 0.02$ rad, ($= 1.1^\circ$). Figure 1 depicts the static positions of robot and human aiming at different goals with crossing paths. We compared the fuzzy approach with the analytical non-fuzzy approach as reference using partitions of $60^\circ, 30^\circ, 15^\circ, 7.5^\circ$ of the unit circle for the orientations with results shown in table I and figures 2-5. Notations in table I are: $\sigma_{z_{1c}}$ - std-computed, $\sigma_{z_{1m}}$ - std-measured etc. The numbers show three general results for the fuzzy approach: **1.** Higher resolution leads to better results. **2.** Method M1 leads to similar results as method M2 for higher resolutions (see also bold numbers in Table I). For low resolutions M1 works better than M2. **3.** The quality of the results regarding measured and computed values depends on the shape of membership functions (mf's). Lower input std's (0.02 rad) require Gaussian mf's, higher input std's (0.05 rad = 2.9°) require Gaussian bell shape mf's which can be explained by different smoothing effects due to different mf-shapes (see columns 4 and 5 in table I). Results 1 and 2 can be explained by the comparison of the corresponding control surfaces and the measurements (black and red dots) to be seen in figures 6 - 10. Figure 6

displays the control surfaces of x_c and y_c for the analytical case (4). The control surfaces of the fuzzy approximations (6) (see [3]) are depicted in figures 7 - 10. Starting from the resolution 60° (fig. 7) we see a very high deviation compared to the analytic approach (fig. 6) which decreases more and more down to resolution 7.5° (fig. 10). This explains the high deviations in standard deviations and correlation coefficients in particular for sector sizes 60° and 30° .

TABLE I
FUZZIFICATION OF THE JACOBIAN J^\dagger

input std	0.02 Gauss, bell shaped (GB)				Gauss	0.05 GB
	sector size/ $^\circ$	60 $^\circ$	30 $^\circ$	15 $^\circ$	7.5 $^\circ$	7.5 $^\circ$
non-fuzzy $\sigma_{z_{1c}}$	0.143	0.140	0.138	0.125	0.144	0.366
fuzzy M1 $\sigma_{z_{1c}}$	0.220	0.184	0.140	0.126	0.144	0.367
fuzzy M2 $\sigma_{z_{1c}}$	0.177	0.190	0.141	0.141	0.142	0.368
non-fuzzy $\sigma_{z_{1m}}$	0.160	0.144	0.138	0.126	0.142	0.368
fuzzy $\sigma_{z_{1m}}$	0.555	0.224	0.061	0.225	0.164	0.381
non-fuzzy $\sigma_{z_{2c}}$	0.128	0.132	0.123	0.114	0.124	0.303
fuzzy M1 $\sigma_{z_{2c}}$	0.092	0.087	0.120	0.112	0.122	0.299
fuzzy M2 $\sigma_{z_{2c}}$	0.160	0.150	0.120	0.119	0.119	0.306
non-fuzzy $\sigma_{z_{2m}}$	0.134	0.120	0.123	0.113	0.129	0.310
fuzzy $\sigma_{z_{2m}}$	0.599	0.171	0.0341	0.154	0.139	0.325
non-fuzzy $\rho_{z_{12c}}$	0.576	0.541	0.588	0.561	0.623	0.669
fuzzy M1 $\rho_{z_{12c}}$	-0.263	0.272	0.478	0.506	0.592	0.592
fuzzy M2 $\rho_{z_{12c}}$	-0.461	0.177	0.481	0.524	0.538	0.535
non-fuzzy $\rho_{z_{12m}}$	0.572	0.459	0.586	0.549	0.660	0.667
fuzzy $\rho_{z_{12m}}$	0.380	0.575	0.990	0.711	0.635	0.592

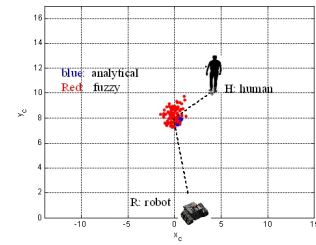


Fig. 2. Sector size: 60 deg

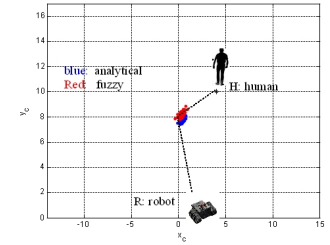


Fig. 3. Sector size: 30 deg

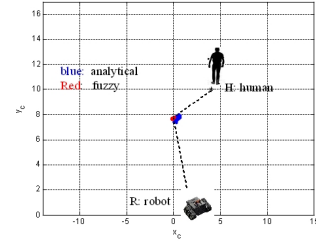


Fig. 4. Sector size: 15 deg

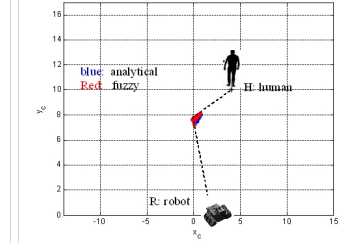


Fig. 5. Sector size: 7.5 deg

VI. DISCUSSIONS AND CONCLUSIONS

We discussed the problem of intersections of trajectories in human-robot systems with respect to uncertainties that are modeled by Gaussian noise on the orientations of human and robot. This problem is solved by a transformation from human-robot orientations to intersection coordinates using a geometrical model and its TS fuzzy version. Based on the input

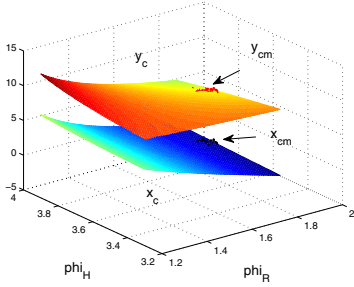


Fig. 6. Control surface non-fuzzy

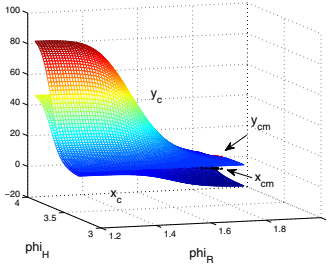


Fig. 7. Control surface fuzzy, 60°

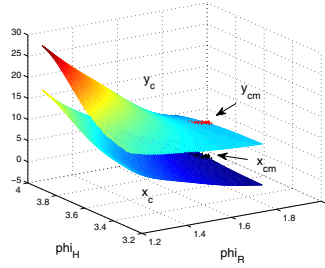


Fig. 8. Control surface fuzzy, 30°

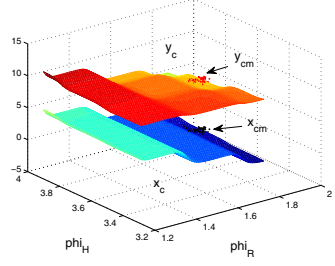


Fig. 9. Control surface fuzzy, 15°

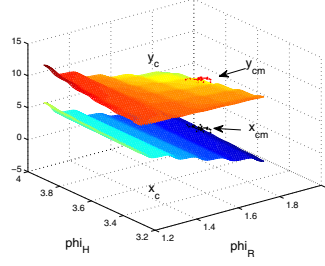


Fig. 10. Control surface fuzzy, 7.5°

standard deviations of the orientations of human and robot, the output standard deviations of the intersection coordinates are calculated. Measurements of the output standard deviations correspond with the calculated values both for the analytical and for the fuzzy approach. We presented two competing methods for fuzzy modeling and extended our method to human/robot positions as well. The analysis based on the two-input case was performed under the condition that the nominal position/orientation of robot and human are constant and known. The measurements of their orientations are distorted by Gaussian noise with known parameters. This analysis together with the fuzzy extension also applies to robots and humans in motion, as long as the positions of robots and humans can be reliably estimated. In further work, by using suitable Kalman filters for the robot and human positions and considering the position estimates for the calculation of the intersections, it is possible to take into account the system noise and the measurement noise at the positions independent of the noise in the orientations. In terms of uncertainties and noise, multiple-robot multiple-person problems ([18], [19], [20], [21]) should

be pairwise solved between a single robot and a single person based on the analysis presented in this paper.

ACKNOWLEDGMENT

This research work has been supported by the AIR-project, Action and Intention Recognition in Human Interaction with Autonomous Systems.

REFERENCES

- [1] O. Khatib. Real-time Obstacle avoidance for manipulators and mobile robots. *IEEE Int. Conf. On Robotics and Automation, St. Louis, Missouri, 1985*, page 500505, 1985.
- [2] J. Firl. Probabilistic maneuver recognition in traffic scenarios. *Doctoral dissertation, KIT Karlsruhe*, 2014.
- [3] R. Palm and A. Lilienthal. Fuzzy logic and control in human-robot systems: geometrical and kinematic considerations. In *WCCI 2018: 2018 IEEE International Conference on Fuzzy Systems (FUZZ-IEEE)*, pages 827–834. IEEE, 2018.
- [4] Karim A. Tahboub. Intelligent human-machine interaction based on dynamic bayesian networks probabilistic intention recognition. *Journal of Intelligent and Robotic Systems*, Volume 45, Issue 1:31–52, 2006.
- [5] T. Fraichard, R. Paulin, and P. Reignier. Human-robot motion: Taking attention into account. *Research Report, RR-8487*, 2014.
- [6] R. Palm, R.T. Chadalavada, and A. Lilienthal. Fuzzy modeling and control for intention recognition in human-robot systems. In *7. IJCCI (FCTA) 2016: Porto, Portugal*, 2016.
- [7] J. Bruce, J. Wawer, and R. Vaughan. Human-robot rendezvous by cooperative trajectory signals. pages 1–2, 2015.
- [8] L. Robertsonsson, B. Iliev, R. Palm, and P. Wide. Perception modeling for human-like artificial sensor systems. *International Journal of Human-Computer Studies* 65 (5), pages 446–459, 2007.
- [9] R. Palm, B. Iliev, and B. Kadmiry. Recognition of human grasps by time-clustering and fuzzy modeling. *Robotics and Autonomous Systems*, Vol. 57, No. 5:484–495, 2009.
- [10] M. Kassner, W.Patera, and A. Bulling. Pupil: an open source platform for pervasive eye tracking and mobile gaze-based interaction. In *Proceedings of the 2014 ACM international joint conference on pervasive and ubiquitous computing*, pages 1151–1160. ACM, 2014.
- [11] R.Palm and D. Driankov. Tuning of scaling factors in fuzzy controllers using correlation functions. In *Proceedings FUZZ-IEEE'93*, San Francisco, California, 1993. IEEE, IEEE.
- [12] P. Banelli. Non-linear transformations of gaussians and gaussian-mixtures with implications on estimation and information theory. *IEEE Trans. on Information Theory*, 2013.
- [13] R.Palm and D. Driankov. Fuzzy inputs. *Fuzzy Sets and Systems - Special issue on modern fuzzy control*, pages 315–335, 1994.
- [14] L.Foulloy and S.Galichet. Fuzzy control with fuzzy inputs. *IEEE Trans. Fuzzy Systems*, 11 (4), pages 437–449, 2003.
- [15] R. Yager and D. B. Filev. Reasoning with probabilistic inputs. In *Proceedings of the Joint Conference of NAFIPS, IFIS and NASA*, pages 352–356, San Antonio, 1994. NAFIPS.
- [16] M. Pota, M.Esposito, and G. De Pietro. Transformation of probability distribution into a fuzzy set interpretable with likelihood view. In *IEEE 11th International Conf. on Hybrid Intelligent Systems (HIS 2011)*, pages 91–96, Malacca Malaysia, 2011. IEEE.
- [17] J.Schaefer and K.Strimmer. A shrinkage to large scale covariance matrix estimation and implications for functional genomics. *Statistical Applications in Genetics and molecular Biology*, vol. 4, iss. 1, Art. 32, 2005.
- [18] J.Alonso-Mora, A. Breitenmoser, M.Rufli, P. Beardsley, and R. Siegwart. Optimal reciprocal collision avoidance for multiple non-holonomic robots. *Proc. of the 10th Intern. Symp. on Distributed Autonomous Robotic Systems (DARS)*, Switzerland, Nov 2010.
- [19] M.S.Goodrich and A.C. Schultz. Humanrobot interaction: A survey. *Foundations and Trends in HumanComputer Interaction*. Vol.1, No.3, page 203275, 2007.
- [20] C.Thorpe T. Fong and C. Baur. Collaboration, dialogue, and human-robot interaction. In *10th International Symposium of Robotics Research*, Lorne, Victoria, Australia, Nov. 2001.
- [21] R. Palm, R.T. Chadalavada, and A. Lilienthal. Recognition of human-robot motion intentions by trajectory observation. In *9th Intern. Conf. on Human System Interaction, HSI2016*. IEEE, 2016.